

Angular Dependence of Specific Heat and Magnetization Effects in the Kitaev Model

Takao Morinari* and Hibiki Takegami†

*Course of Studies on Materials Science, Graduate School of Human
and Environmental Studies, Kyoto University, Kyoto 606-8501, Japan*

(Dated: March 11, 2025)

We investigate the effect of a magnetic field on the Kitaev model using the equation of motion approach for the spin Green's function. Our study considers both cases: suppressed magnetization and finite magnetization in the paramagnetic phase of the Kitaev model. When magnetization is suppressed, the specific heat exhibits an angular dependence with a 60° periodicity, consistent with recent experimental observations in α -RuCl₃. This behavior can be interpreted as a signature of Majorana fermion gap formation. However, when magnetization is included, the periodicity shifts from 60° to 180° , suggesting that the Majorana fermion gap behavior is no longer present in this regime. Our results indicate that the suppression of magnetization is essential for observing features associated with Majorana fermions, suggesting that a nearest-neighbor antiferromagnetic interaction could contribute to this suppression.

I. INTRODUCTION

The Kitaev model [1], a paradigmatic example of exactly solvable quantum spin liquid systems, has attracted significant attention in condensed matter physics due to its potential to host non-Abelian anyons and topologically protected quantum states [2–4]. One of the most compelling approaches to studying the Kitaev model is through the formalism of Majorana fermions [1, 5–7], which maps spin degrees of freedom onto itinerant and localized fermionic ones, enabling an exact solution at zero temperature.

The physics of the Kitaev model can be explored in real materials [8–11], where the dominant interaction is the Kitaev interaction mediated via the Jackeli-Khaliullin mechanism [12]. Among these materials, α -RuCl₃ [13] has emerged as one of the most studied examples. This material exhibits a zigzag magnetic order [14, 15] due to non-Kitaev interactions [16–18]. This magnetic order is suppressed by applying a magnetic field of approximately 7T [19, 20], leading to the emergence of a paramagnetic state, where half-quantized thermal Hall conductivity has been observed [21–24]. This half-integer quantization is often attributed to the chiral edge modes of Majorana fermions, with the itinerant Majorana fermions in the B-phase becoming gapped under an applied magnetic field [1]. The magnetic field angle dependence of heat capacity [25] further supports this gap in the Majorana fermions. However, the presence of the chiral Majorana edge mode with a well-defined Chern number remains unsettled, as experiments [26, 27] report that the thermal Hall conductivity does not show any plateau.

To theoretically investigate the Kitaev spin liquid phase in real materials, it is crucial to account for the effects of the magnetic field [28, 29], as it is necessary to suppress the magnetic orders in these systems. Exact

diagonalization studies [30, 31] have shown the presence of the Kitaev spin liquid phase under a magnetic field, with phase boundaries determined by the second derivative of the ground state energy and fidelity susceptibility. Similarly, density-matrix renormalization group methods have been applied to study the Kitaev model, including non-Kitaev interactions, revealing spin liquid phases in both ferromagnetic and antiferromagnetic Kitaev interactions [32–35]. However, as suggested by the tensor-network method [36], identifying the Kitaev spin liquid phase requires taking the thermodynamic limit.

In this paper, we employ the equation of motion approach for the spin Green's function, a method that is both free from finite-size effects and non-perturbative. This approach is particularly well-suited for investigating properties in the thermodynamic limit. We have previously applied this method to the pure Kitaev model [37, 38], obtaining results that are largely consistent with Majorana-based numerical simulations [39]. In the present work, we extend our analysis to include the effect of the magnetic field, focusing on the signatures of Majorana fermions while using spin operators rather than relying on the Majorana representation. Since we are interested in the gap formation in the Majorana fermion spectrum, we analyze the magnetic field angle dependence of the specific heat, comparing our findings with experimental observations [25]. We find that the results are consistent with experiment when the paramagnetic magnetization is suppressed. However, we also observe that the presence of magnetization in the paramagnetic phase suppresses the periodicity associated with the Chern number. Our study suggests that non-Kitaev interactions, particularly nearest-neighbor antiferromagnetic interactions, may play a crucial role in stabilizing the Kitaev spin liquid phase. Another possibility is the antiferromagnetic Kitaev model, where the effect of magnetization is naturally suppressed, potentially facilitating the emergence of the spin liquid phase.

The remainder of the paper is organized as follows. In Sec. II, we introduce the equation of motion approach for the Kitaev model under a magnetic field. In Sec. III, we

* morinari.takao.5s@kyoto-u.ac.jp

† takegami.hibiki.64h@st.kyoto-u.ac.jp

present results for the case where magnetization is suppressed, demonstrating that the periodicity in the angular dependence of the specific heat matches the experimental observations. In Sec. IV, we discuss the results when the magnetic field effect is fully taken into account, highlighting how the presence of magnetization suppresses the features associated with the gap in the Majorana fermions. Finally, Sec. V summarizes our findings. The algorithm for solving the self-consistent equations is provided in Appendix A.

II. FORMALISM

We consider the Kitaev model on a honeycomb lattice, as depicted in Fig. 1, under the influence of a uniform magnetic field $\mathbf{b} = (b_x, b_y, b_z)$. The Hamiltonian is given by

$$H = - \sum_{\gamma=x,y,z} J_\gamma \sum_{\langle i,j \rangle_\gamma} S_i^\gamma S_j^\gamma - \sum_j (b_x S_j^x + b_y S_j^y + b_z S_j^z), \quad (1)$$

where S_j^γ represents the γ -component of the spin-1/2 operator at site j and $\langle i,j \rangle_\gamma$ refers to the nearest-neighbor sites i and j connected by a bond in the γ -direction. For example, in Fig. 1, the bond connecting site 0 and site 1 is an x -bond, the bond between site 0 and site 2 is a y -bond, and the bond between site 0 and site 3 is a z -bond. The other γ -bonds are parallel to these, respectively. For convenience, the lattice sites on the honeycomb lattice are labeled as shown in Fig. 1.

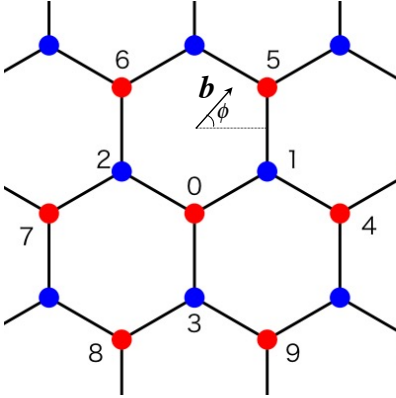


FIG. 1. Honeycomb lattice structure in the Kitaev model. To aid in the presentation of the Green's function formalism and the derivation of the equations of motion, several lattice sites are numbered for clarity. The arrow indicates the direction of the applied magnetic field \mathbf{b} . The angle ϕ is measured from the horizontal axis, as shown in the figure.

To investigate the spin correlations in the Kitaev model, we define the following Matsubara Green's function:

$$G_{0,j}^{\gamma_1 \gamma_2}(\tau) = - \langle T_\tau S_0^{\gamma_1}(\tau) S_j^{\gamma_2}(0) \rangle \equiv \langle S_0^{\gamma_1} | S_j^{\gamma_2} \rangle_\tau, \quad (2)$$

where τ denotes the imaginary time, and T_τ is the imaginary-time ordering operator. Hereafter, for any operator A , we define its imaginary-time dependence as

$$A(\tau) = e^{\tau H} A e^{-\tau H}. \quad (3)$$

We define the Fourier transform of $G_{0,j}^{\gamma_1 \gamma_2}(\tau)$ as

$$G_{0,j}^{\gamma_1 \gamma_2}(i\omega_n) = \int_0^\beta d\tau e^{i\omega_n \tau} G_{0,j}^{\gamma_1 \gamma_2}(\tau) \equiv \langle S_0^{\gamma_1} | S_j^{\gamma_2} \rangle_{i\omega_n}. \quad (4)$$

Here, $\beta = 1/T$ is the inverse temperature, where T denotes the temperature, and the Boltzmann constant is set to $k_B = 1$. The bosonic Matsubara frequency is given by $\omega_n = 2\pi n/\beta$, where n is an integer.

To analyze this Green's function, we consider its equation of motion, given by [40, 41]:

$$i\omega_n \langle S_0^{\gamma_1} | S_j^{\gamma_2} \rangle_{i\omega_n} = \langle [S_0^{\gamma_1}, H] | S_j^{\gamma_2} \rangle_{i\omega_n} + \langle [S_0^{\gamma_1}, S_j^{\gamma_2}] \rangle. \quad (5)$$

From this equation, it is clear that this approach has a hierarchical structure. To solve this equation, we need the equation of motion of the Green's function, which appears as the first term on the right-hand side. This equation of motion is obtained by replacing $S_0^{\gamma_1}$ with $[S_0^{\gamma_1}, H]$ in Eq. (5). This process generates additional Green's functions. To close the set of equations, we need to introduce an approximation. Below, we will apply the Tyablikov decoupling approximation to achieve this.

Computing $[S_0^{\gamma_1}, H]$ in Eq. (5), where the Hamiltonian is given by Eq. (1), we obtain, for the case of $\gamma_1 = \gamma_2 = x$:

$$i\omega_n \langle S_0^x | S_j^x \rangle_{i\omega_n} = -iJ_y \langle S_0^z S_2^y | S_j^x \rangle_{i\omega_n} + iJ_z \langle S_0^y S_3^z | S_j^x \rangle_{i\omega_n} - ib_y \langle S_0^z | S_j^x \rangle_{i\omega_n} + ib_z \langle S_0^y | S_j^x \rangle_{i\omega_n}. \quad (6)$$

This is referred to as the first-order equation of motion. Next, we obtain the second equation of motion for the first and second terms on the right-hand side of Eq. (6) as follows:

$$\begin{aligned} i\omega_n \langle S_0^z S_2^y | S_j^x \rangle_{i\omega_n} &= -iJ_x \langle S_0^y S_1^x S_2^y | S_j^x \rangle_{i\omega_n} - iJ_z \langle S_0^z S_2^x S_6^z | S_j^x \rangle_{i\omega_n} \\ &+ iJ_x \langle S_0^z S_2^z S_7^x | S_j^x \rangle_{i\omega_n} + \frac{iJ_y}{4} \langle S_0^x | S_j^x \rangle_{i\omega_n} \\ &+ ib_x \langle S_0^z S_2^z | S_j^x \rangle_{i\omega_n} - ib_x \langle S_0^y S_2^y | S_j^x \rangle_{i\omega_n} \\ &+ ib_y \langle S_0^x S_2^x | S_j^x \rangle_{i\omega_n} - ib_z \langle S_0^z S_2^z | S_j^x \rangle_{i\omega_n} \\ &+ i\delta_{0,j} \langle S_0^y S_2^y \rangle - i\delta_{2,j} \langle S_0^z S_2^z \rangle, \end{aligned} \quad (7)$$

and

$$\begin{aligned} i\omega_n \langle S_0^y S_3^z | S_j^x \rangle_{i\omega_n} &= iJ_x \langle S_0^z S_1^x S_3^z | S_j^x \rangle_{i\omega_n} - iJ_x \langle S_0^y S_3^y S_8^x | S_j^x \rangle_{i\omega_n} \\ &+ iJ_y \langle S_0^y S_3^x S_9^y | S_j^x \rangle_{i\omega_n} - \frac{iJ_z}{4} \langle S_0^x | S_j^x \rangle_{i\omega_n} \\ &+ ib_x \langle S_0^z S_3^z | S_j^x \rangle_{i\omega_n} - ib_z \langle S_0^x S_3^x | S_j^x \rangle_{i\omega_n} \\ &- ib_x \langle S_0^y S_3^y | S_j^x \rangle_{i\omega_n} + ib_y \langle S_0^x S_3^x | S_j^x \rangle_{i\omega_n} \\ &- i\delta_{0,j} \langle S_0^z S_3^z \rangle + i\delta_{3,j} \langle S_0^y S_3^y \rangle. \end{aligned} \quad (8)$$

By combining these two Green's functions, we define the following Green's function:

$$F_{0,j}^{xx}(i\omega_n) = -iJ_y \langle S_0^z S_2^y | S_j^x \rangle_{i\omega_n} + iJ_z \langle S_0^y S_3^z | S_j^x \rangle_{i\omega_n}, \quad (9)$$

with its corresponding equation of motion:

$$\begin{aligned} i\omega_n F_{0,j}^{xx}(i\omega_n) &= -J_x J_y \langle S_0^y S_1^x S_2^y | S_j^x \rangle_{i\omega_n} - J_y J_z \langle S_0^z S_2^x S_6^z | S_j^x \rangle_{i\omega_n} \\ &+ J_x J_y \langle S_0^z S_2^z S_7^x | S_j^x \rangle_{i\omega_n} - J_x J_z \langle S_0^z S_1^x S_3^z | S_j^x \rangle_{i\omega_n} \\ &+ J_x J_z \langle S_0^y S_3^y S_8^x | S_j^x \rangle_{i\omega_n} - J_y J_z \langle S_0^y S_3^x S_9^y | S_j^x \rangle_{i\omega_n} \\ &- J_y b_x \langle S_0^y S_2^y | S_j^x \rangle_{i\omega_n} + J_y b_y \langle S_0^x S_2^y | S_j^x \rangle_{i\omega_n} \\ &- J_z b_x \langle S_0^z S_3^z | S_j^x \rangle_{i\omega_n} + J_z b_z \langle S_0^x S_3^z | S_j^x \rangle_{i\omega_n} \\ &+ J_y b_x \langle S_0^z S_2^z | S_j^x \rangle_{i\omega_n} - J_y b_z \langle S_0^z S_2^x | S_j^x \rangle_{i\omega_n} \\ &+ J_z b_x \langle S_0^y S_3^y | S_j^x \rangle_{i\omega_n} - J_z b_y \langle S_0^y S_3^x | S_j^x \rangle_{i\omega_n} \\ &+ \frac{J_y^2 + J_z^2}{4} \langle S_0^x | S_j^x \rangle_{i\omega_n} + J_y \delta_{0,j} \langle S_0^y S_2^y \rangle - J_y \delta_{2,j} \langle S_0^z S_2^z \rangle \\ &+ J_z \delta_{0,j} \langle S_0^z S_3^z \rangle - J_z \delta_{3,j} \langle S_0^y S_3^y \rangle. \end{aligned} \quad (10)$$

We now apply the decoupling approximation to the four-spin Green's functions appearing on the right-hand side of Eq. (10). There are several ways to approximate these Green's functions in terms of the product of a spin correlation function and a Green's function with fewer spin. Our strategy is to choose the decoupling method that retains the strongest correlations. For instance, we approximate the Green's function $\langle S_0^y S_1^x S_2^y | S_j^x \rangle_{i\omega_n}$ in the following way:

$$\langle S_0^y S_1^x S_2^y | S_j^x \rangle_{i\omega_n} \simeq \alpha \langle S_0^y S_2^y \rangle \langle S_1^x | S_j^x \rangle_{i\omega_n}, \quad (11)$$

where the parameter α is introduced to improve the accuracy of the approximation. While there are alternative ways to extract spin correlation functions, the correlation function $\langle S_0^y S_2^y \rangle$ is dominant compared to other correlation functions. Furthermore, the Green's function $\langle S_1^x | S_j^x \rangle_{i\omega_n}$ describes the largest correlation in the Kitaev model when $j = 0$ or $j = 1$. For other Green's functions, a similar decoupling approximation can be applied, though the correlations are weaker. For instance, the Green's function $\langle S_0^z S_2^x S_6^z | S_j^x \rangle_{i\omega_n}$ can be approximated as:

$$\langle S_0^z S_2^x S_6^z | S_j^x \rangle_{i\omega_n} \simeq \langle S_0^z S_6^z \rangle \langle S_2^x | S_j^x \rangle_{i\omega_n}. \quad (12)$$

Here, we note that the correlation function $\langle S_0^z S_6^z \rangle$ is significantly weaker compared to $\langle S_0^y S_2^y \rangle$. Additionally, Green's functions containing three spins appear in the formalism, but their inclusion would correspond to higher-order contributions. Therefore, we restrict our analysis to second-order approximation and neglect the higher-order contributions. Furthermore, in the self-consistent equations below, we set $j = 0$ or $j = 1$. Within the Kitaev interaction framework, these Green's functions describe weaker spin-spin correlations

than $\langle S_0^x | S_j^x \rangle_{i\omega_n}$, $\langle S_0^z S_2^y | S_j^x \rangle_{i\omega_n}$, and $\langle S_0^y S_3^z | S_j^x \rangle_{i\omega_n}$. These weaker correlations are safely neglected within the second-order approximation. Applying these approximations, we obtain:

$$\begin{aligned} i\omega_n F_{0,j}^{xx}(i\omega_n) &\simeq + \frac{J_y^2 + J_z^2}{4} \langle S_0^x | S_j^x \rangle_{i\omega_n} \\ &- \alpha J_x (J_y c_y + J_z c_z) \langle S_1^x | S_j^x \rangle_{i\omega_n} \\ &+ (J_y c_y + J_z c_z) \delta_{0,j}. \end{aligned} \quad (13)$$

Here, the correlation functions are defined as

$$c_\gamma = \langle S_0^\gamma S_{\delta_\gamma}^\gamma \rangle, \quad (14)$$

where $\delta_x = 1$, $\delta_y = 2$, and $\delta_z = 3$. We also derive the equation of motion for $\langle S_0^y | S_j^x \rangle_{i\omega_n}$ and $\langle S_0^z | S_j^x \rangle_{i\omega_n}$, which appear on the right-hand side of Eq. (6), while incorporating the approximations above. This leads to a set of coupled equations:

$$i\omega_n G_{0,j}^{xx}(i\omega_n) = F_{0,j}^{xx}(i\omega_n) - ib_y G_{0,j}^{zx}(i\omega_n) + ib_z G_{0,j}^{yx}(i\omega_n) \quad (15)$$

$$i\omega_n G_{0,j}^{yx}(i\omega_n) = -ib_z G_{0,j}^{xx}(i\omega_n) + ib_x G_{0,j}^{zx}(i\omega_n) - i\delta_{0,j} m_z \quad (16)$$

$$i\omega_n G_{0,j}^{zx}(i\omega_n) = -ib_x G_{0,j}^{yx}(i\omega_n) + ib_y G_{0,j}^{xx}(i\omega_n) + i\delta_{0,j} m_y \quad (17)$$

$$\begin{aligned} i\omega_n F_{0,j}^{xx}(i\omega_n) &= -J_x \alpha (J_y c_y + J_z c_z) G_{1,j}^{xx}(i\omega_n) \\ &+ \frac{J_y^2 + J_z^2}{4} G_{0,j}^{xx}(i\omega_n) + \delta_{0,j} (J_y c_y + J_z c_z). \end{aligned} \quad (18)$$

Since the fourth equation contains $G_{1,j}^{xx}(i\omega_n)$, we require its equation of motion. Expanding it up to second order in a similar manner, we obtain:

$$i\omega_n G_{1,j}^{xx}(i\omega_n) = F_{1,j}^{xx}(i\omega_n) - ib_y G_{1,j}^{zx}(i\omega_n) + ib_z G_{1,j}^{yx}(i\omega_n) \quad (19)$$

$$i\omega_n G_{1,j}^{yx}(i\omega_n) = ib_x G_{1,j}^{zx}(i\omega_n) - ib_z G_{1,j}^{xx}(i\omega_n) - i\delta_{1,j} m_z \quad (20)$$

$$i\omega_n G_{1,j}^{zx}(i\omega_n) = -ib_x G_{1,j}^{yx}(i\omega_n) + ib_y G_{1,j}^{xx}(i\omega_n) + i\delta_{1,j} m_y \quad (21)$$

$$\begin{aligned} i\omega_n F_{1,j}^{xx}(i\omega_n) &= -J_x \alpha (J_y c_y + J_z c_z) G_{0,j}^{xx}(i\omega_n) \\ &+ \frac{J_y^2 + J_z^2}{4} G_{1,j}^{xx}(i\omega_n) + \delta_{1,j} (J_y c_y + J_z c_z), \end{aligned} \quad (22)$$

where:

$$F_{1,j}^{xx}(i\omega_n) = -iJ_y \langle S_1^z S_4^y | S_j^x \rangle_{i\omega_n} + iJ_z \langle S_1^y S_5^z | S_j^x \rangle_{i\omega_n}. \quad (23)$$

To compute c_y and c_z , we require a similar set of equations for $G_{0,j}^{yy}(i\omega_n)$ and $G_{0,j}^{zz}(i\omega_n)$. These can be derived from the above equations by applying the cyclic permutation: $x \rightarrow y \rightarrow z \rightarrow x$, $1 \rightarrow 2 \rightarrow 3 \rightarrow 1$.

The set of equations of motion is summarized in the following equation:

$$i\omega_n \mathbf{G}^\gamma (i\omega_n) = M^\gamma \mathbf{G}^\gamma (i\omega_n) + \mathbf{c}^\gamma, \quad (24)$$

where

$$\mathbf{G}^x (i\omega_n) = (G_{0,0}^{xx} \ G_{0,0}^{yx} \ G_{0,0}^{zx} \ F_{0,0}^{xx} \ G_{1,0}^{xx} \ G_{1,0}^{yx} \ G_{1,0}^{zx} \ F_{1,0}^{xx})^T, \quad (25)$$

$$\mathbf{G}^y (i\omega_n) = (G_{0,0}^{yy} \ G_{0,0}^{zy} \ G_{0,0}^{xy} \ F_{0,0}^{yy} \ G_{2,0}^{yy} \ G_{2,0}^{zy} \ G_{2,0}^{xy} \ F_{2,0}^{yy})^T, \quad (26)$$

$$\mathbf{G}^z (i\omega_n) = (G_{0,0}^{zz} \ G_{0,0}^{xz} \ G_{0,0}^{yz} \ F_{0,0}^{zz} \ G_{3,0}^{zz} \ G_{3,0}^{xz} \ G_{3,0}^{yz} \ F_{3,0}^{zz})^T. \quad (27)$$

Note that the dependence on $i\omega_n$ in the right-hand side of these equations is implicit. The matrices M^x , M^y , and M^z are given by

$$M^x = \begin{pmatrix} 0 & ib_z & -ib_y & 1 & 0 & 0 & 0 & 0 \\ -ib_z & 0 & ib_x & 0 & 0 & 0 & 0 & 0 \\ ib_y & -ib_x & 0 & 0 & 0 & 0 & 0 & 0 \\ \frac{1}{4}(J_y^2 + J_z^2) & 0 & 0 & 0 & -J_x\alpha(J_y c_y + J_z c_z) & 0 & 0 & 0 \\ 0 & 0 & 0 & 0 & 0 & ib_z & -ib_y & 1 \\ 0 & 0 & 0 & 0 & -ib_z & 0 & ib_x & 0 \\ 0 & 0 & 0 & 0 & ib_y & -ib_x & 0 & 0 \\ -J_x\alpha(J_y c_y + J_z c_z) & 0 & 0 & 0 & \frac{1}{4}(J_y^2 + J_z^2) & 0 & 0 & 0 \end{pmatrix}, \quad (28)$$

$$M^y = \begin{pmatrix} 0 & ib_x & -ib_z & 1 & 0 & 0 & 0 & 0 \\ -ib_x & 0 & ib_y & 0 & 0 & 0 & 0 & 0 \\ ib_z & -ib_y & 0 & 0 & 0 & 0 & 0 & 0 \\ \frac{1}{4}(J_z^2 + J_x^2) & 0 & 0 & 0 & -J_y\alpha(J_z c_z + J_x c_x) & 0 & 0 & 0 \\ 0 & 0 & 0 & 0 & 0 & ib_x & -ib_z & 1 \\ 0 & 0 & 0 & 0 & -ib_x & 0 & ib_y & 0 \\ 0 & 0 & 0 & 0 & ib_z & -ib_y & 0 & 0 \\ -J_y\alpha(J_z c_z + J_x c_x) & 0 & 0 & 0 & \frac{1}{4}(J_z^2 + J_x^2) & 0 & 0 & 0 \end{pmatrix}, \quad (29)$$

$$M^z = \begin{pmatrix} 0 & ib_y & -ib_x & 1 & 0 & 0 & 0 & 0 \\ -ib_y & 0 & ib_z & 0 & 0 & 0 & 0 & 0 \\ ib_x & -ib_z & 0 & 0 & 0 & 0 & 0 & 0 \\ \frac{1}{4}(J_x^2 + J_y^2) & 0 & 0 & 0 & -J_z\alpha(J_x c_x + J_y c_y) & 0 & 0 & 0 \\ 0 & 0 & 0 & 0 & 0 & ib_y & -ib_x & 1 \\ 0 & 0 & 0 & 0 & -ib_y & 0 & ib_z & 0 \\ 0 & 0 & 0 & 0 & ib_x & -ib_z & 0 & 0 \\ -J_z\alpha(J_x c_x + J_y c_y) & 0 & 0 & 0 & \frac{1}{4}(J_x^2 + J_y^2) & 0 & 0 & 0 \end{pmatrix}. \quad (30)$$

The vectors \mathbf{c}^x , \mathbf{c}^y , and \mathbf{c}^z are defined as

$$\mathbf{c}^x = (0 \ -im_z \ im_y \ J_y c_y + J_z c_z \ 0 \ 0 \ 0 \ 0)^T, \quad (31)$$

$$\mathbf{c}^y = (0 \ +im_z \ -im_x \ J_z c_z + J_x c_x \ 0 \ 0 \ 0 \ 0)^T, \quad (32)$$

$$\mathbf{c}^z = (0 \ -im_y \ im_x \ J_x c_x + J_y c_y \ 0 \ 0 \ 0 \ 0)^T, \quad (33)$$

where

$$m_\gamma = \langle S_0^\gamma \rangle. \quad (34)$$

We note that in the paramagnetic phase, we may set

$$(m_x, m_y, m_z) = \frac{\mathbf{b}}{|\mathbf{b}|} m. \quad (35)$$

Therefore, the quantity to be self-consistently determined is m , rather than each individual component m_γ .

The self-consistent equation is conveniently expressed in terms of the imaginary-time Green's function,

$$\mathbf{G}^\gamma(\tau) = \frac{1}{\beta} \sum_{i\omega_n} e^{-i\omega_n \tau} \mathbf{G}^\gamma(i\omega_n), \quad (36)$$

as

$$[\mathbf{G}^\gamma (\tau = +0)]_0 = -\langle S_0^\gamma S_0^\gamma \rangle = -\frac{1}{4}, \quad (37)$$

$$[\mathbf{G}^\gamma (\tau = +0)]_4 = -\langle S_{\delta_\gamma}^\gamma S_0^\gamma \rangle = -c_\gamma. \quad (38)$$

Note that there are six equations, while the number of parameters to be determined is five: c_x , c_y , c_z , α , and m . For the case of $J_x = J_y \neq J_z$, the formulation can be extended by introducing two different parameters, α_x and α_z , instead of a single parameter α . However, in this study, we use a single parameter α to solve the self-consistent equations, and we select five equations out of the six available. Specifically, we use the three equations given by Eq. (37) and the two equations from Eq. (38) with $\gamma = x, y$. In Appendix A, we provide details on how to solve the Green's function equations in the matrix form given by Eq. (24).

III. MAGNETIC FIELD EFFECTS UNDER CONSERVED \mathbb{Z}_2 GAUGE FLUXES

Kitaev explored the effect of time-reversal symmetry breaking in the B-phase to explain the gap opening in massless Majorana fermions [1]. In this approach, the effect of the magnetic field was treated perturbatively, while restricting the Hilbert space to configurations that do not contain free \mathbb{Z}_2 gauge fluxes. Due to this restriction, the first-order term in the magnetic field expansion vanishes, and the time-reversal symmetry breaking term appears at third order. In our formalism, we can reproduce this scenario by suppressing the magnetization, which corresponds to setting $m = 0$.

In our study, we focus on the properties associated with the spin-liquid phase, specifically examining the magnetic field direction dependence of the spin correlations. Inspired by the experimental work in [25], we analyze the angular dependence of the specific heat to explore how the magnetic field influences the gap formation. For α - RuCl_3 , the unit vectors along the a-axis and b-axis are given by

$$\mathbf{e}_a = \frac{1}{\sqrt{6}}(1, 1, -2), \quad (39)$$

$$\mathbf{e}_b = \frac{1}{\sqrt{2}}(-1, 1, 0), \quad (40)$$

respectively. In Fig. 1, the horizontal direction is parallel to \mathbf{e}_a , while the vertical direction is parallel to \mathbf{e}_b . If we define the angle ϕ of the magnetic field as shown in Fig. 1, then

$$\mathbf{b} = b(\mathbf{e}_a \cos \phi + \mathbf{e}_b \sin \phi). \quad (41)$$

Thus,

$$b_x = \left(\frac{1}{\sqrt{6}} \cos \phi - \frac{1}{\sqrt{2}} \sin \phi \right) b, \quad (42)$$

$$b_y = \left(\frac{1}{\sqrt{6}} \cos \phi + \frac{1}{\sqrt{2}} \sin \phi \right) b, \quad (43)$$

$$b_z = -\frac{2}{\sqrt{6}} b \cos \phi. \quad (44)$$

In solving the self-consistent equation, we first solve it at high temperature, $T \sim 10J_\gamma$, where the initial values are taken from the high-temperature expansion (HTE) as follows:

$$\langle S_0^x S_1^x \rangle_{\text{HTE}} = \frac{J_x \beta}{16} + \frac{b_x^2 \beta^2}{16} + O(\beta^3), \quad (45)$$

$$\langle S_0^y S_2^y \rangle_{\text{HTE}} = \frac{J_y \beta}{16} + \frac{b_y^2 \beta^2}{16} + O(\beta^3), \quad (46)$$

$$\langle S_0^z S_3^z \rangle_{\text{HTE}} = \frac{J_z \beta}{16} + \frac{b_z^2 \beta^2}{16} + O(\beta^3), \quad (47)$$

where $\langle \dots \rangle_{\text{HTE}}$ denotes the expectation value obtained from HTE. For the parameter α , we compute the following quantity:

$$\begin{aligned} \alpha_{\text{HTE}}^{xy} &= \frac{\langle S_0^y S_1^x S_2^y S_3^x \rangle_{\text{HTE}}}{\langle S_0^y S_2^y \rangle_{\text{HTE}} \langle S_1^x S_3^x \rangle_{\text{HTE}}} \\ &= 1 + \beta \left(-\frac{J_x}{2} - \frac{b_y^2}{J_y} \right) \\ &\quad + \beta^2 \left(-\frac{J_y^2}{96} + \frac{J_x^2}{4} + \frac{J_x b_y^2}{2J_y} + \frac{b_y^4}{J_y^2} \right) + O(\beta^3). \end{aligned} \quad (48)$$

Note that the right-hand side depends on J_x , J_y , J_z , and the components of the magnetic field. There are five other similar quantities; however, we take the average of all six quantities and use this as the initial value of α . In the following calculations, we focus on the isotropic case, where $J_x = J_y = J_z \equiv J$, and take J as the unit of energy.

Figure 2 shows the temperature dependence of the spin correlation functions and the parameter α at $b = 0.2$ and $\phi = 40^\circ$. From Fig. 2(a), we observe that anisotropy in the correlation functions emerges at low temperatures. At temperatures above ~ 0.5 , the correlation functions remain nearly isotropic, as confirmed by the temperature dependence of their differences shown in Fig. 2(b). Meanwhile, we find that $\alpha \sim 1$ at high temperatures, as shown in the inset of Fig. 2(a). This indicates that the decoupling approximation is accurate at high temperatures.

We now investigate the angle ϕ dependence of the spin correlations. We start from the solution at a given temperature and ϕ , using this solution as the initial condition, and then solve the self-consistent equations while gradually increasing ϕ . Figure 3 shows the ϕ dependence of the spin correlation functions and energy at $b = 0.2$

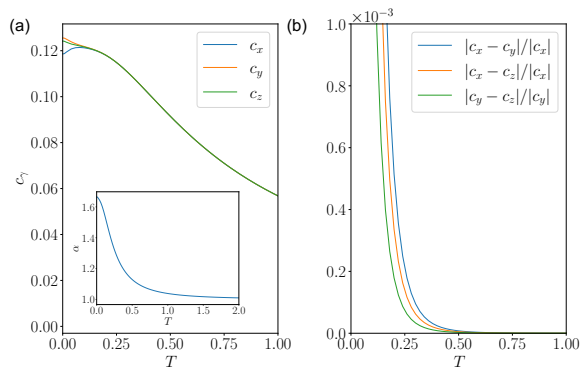


FIG. 2. (a) Temperature dependence of the spin correlation functions c_x , c_y , and c_z . The inset shows the temperature dependence of the decoupling parameter α , which is introduced in the decoupling approximation. (b) Temperature dependence of the differences in the spin correlation functions. Both (a) and (b) are computed for $b = 0.2$ and $\phi = 40^\circ$, where the magnetic field components are given by $b_x = -0.028$, $b_y = 0.153$, and $b_z = -0.125$.

and $T = 0.01$. The ϕ dependence of the spin correlation functions, shown in Fig. 3(a), can be approximately understood in terms of the quantity $\tilde{b}_\gamma \equiv |b_\gamma|/|\mathbf{b}|$, which is plotted in Fig. 3(b). The correlation function c_γ reaches its minimum values when $\tilde{b}_\gamma = 0$. The energy per site can be computed as:

$$E = -\frac{1}{2}J(c_x + c_y + c_z). \quad (49)$$

Figure 3(c) shows the ϕ dependence of E . We observe a clear 60° periodicity, although the amplitude is quite small. Figure 4 presents the ϕ dependence of the poles of the Green's function, $\mathbf{G}^\gamma(i\omega_n)$, denoted as $E_\gamma(\phi)$. Notably, zero-energy poles appear in $\mathbf{G}^\gamma(i\omega_n)$ when $b_\gamma = 0$. However, the behavior of the spin correlation functions cannot be fully explained by \tilde{b}_γ alone. In fact, the difference between the spin correlations and \tilde{b}_γ leads to the ϕ dependence of the energy, as shown in Fig. 3(c). The specific heat is obtained by taking the temperature derivative of the energy. Figure 5 presents the ϕ dependence of the specific heat at $T = 0.01$ for different magnetic fields. The specific heat exhibits a 60° periodicity, and the amplitude increases with increasing magnetic field. This 60° periodicity is consistent with experimental results reported for α -RuCl₃ in Ref. [25].

The angular dependence of the energy and specific heat implies a nontrivial interplay between the spin correlations in the Kitaev model and the magnetic field. From the perspective of fractionalized Majorana fermions, the gapless Majorana fermions acquire a gap in the presence of a magnetic field, and this gap is proportional to $|b_x b_y b_z| \propto |\cos 3\phi|$. As a result, the Majorana fermions remain gapless when $\phi = 30^\circ + 60^\circ \times n$, while the gap is maximized at $\phi = 60^\circ \times n$, where n is an integer. When the Majorana fermions are gapped, the specific heat decreases exponentially with decreasing temperature. In

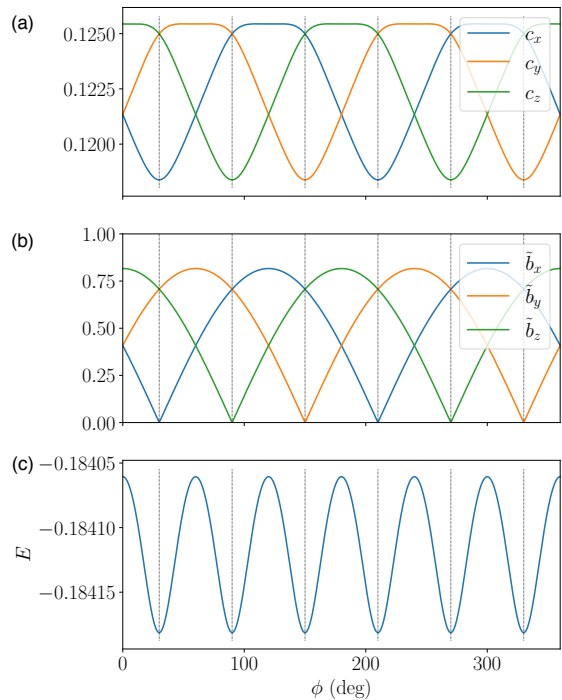


FIG. 3. (a) Angular dependence of the spin correlation functions, and (b) the dependence of $\tilde{b}_\gamma = |b_\gamma|/|\mathbf{b}|$ on the angle ϕ for $\gamma = x, y, z$, at $b = 0.2$ and $T = 0.01$. (c) Energy per site as a function of the angle ϕ . The vertical lines represent the angles $\phi = 30^\circ + 60^\circ \times n$, where n is an integer.

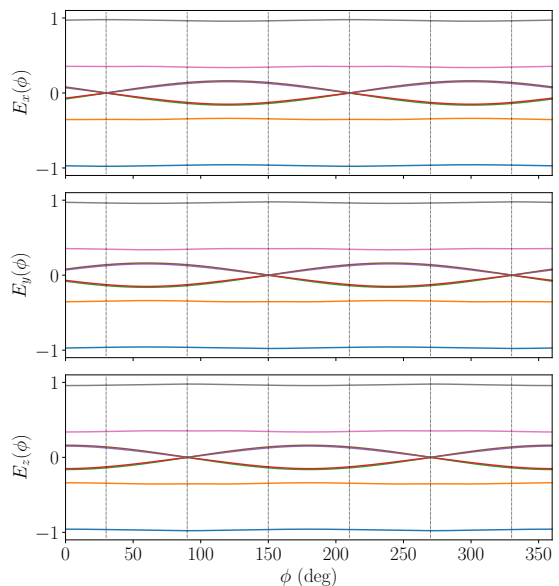


FIG. 4. Angular dependence of the poles of the Green's function $\mathbf{G}^\gamma(i\omega_n)$, denoted as $E_\gamma(\phi)$, at $b = 0.2$ and $T = 0.01$. Zero-energy poles appear when $b_\gamma = 0$, indicating points where the gap closes.

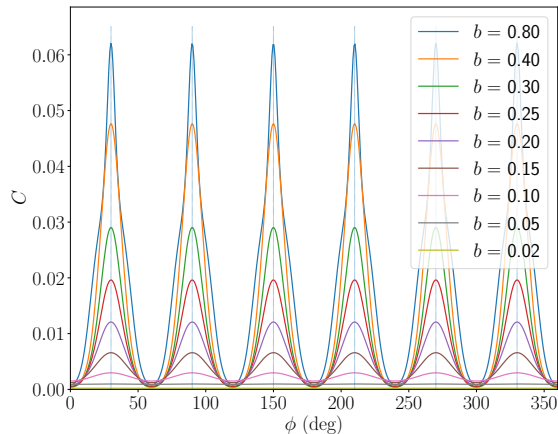


FIG. 5. Angular dependence of the specific heat at $T = 0.01$ for different magnetic fields. The vertical lines indicate specific angles as described earlier.

contrast, when the Majorana fermions remain gapless, the specific heat follows a T^2 dependence at low temperatures. Figure 6 shows the temperature dependence of C/T for different magnetic field strengths along (a) the $\phi = 0^\circ$ direction and (b) the $\phi = 90^\circ$ direction. We observe a qualitative difference between the two cases. However, we do not observe a clear linear temperature dependence in C/T for $\phi = 90^\circ$. This is likely due to the limitations of our approach at low temperatures, where its accuracy may not be sufficient.

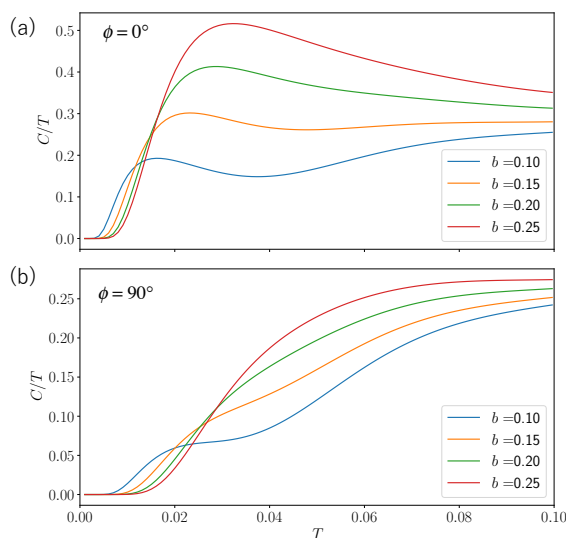


FIG. 6. Temperature dependence of C/T for various magnetic field strengths along (a) the $\phi = 0^\circ$ direction and (b) the $\phi = 90^\circ$ direction.

IV. FULL MAGNETIC FIELD EFFECTS ON THE KITAEV MODEL

Now, we consider the full magnetic field effect on the Kitaev model. When the magnetization is included, the system exhibits qualitatively different behavior. In solving the self-consistent equations (37) and (38), we take the initial value of $m = \sqrt{m_x^2 + m_y^2 + m_z^2}$ from the HTE. Specifically, we obtain it from the HTE of m_γ ($\gamma = x, y, z$):

$$m_\gamma^{\text{HTE}} = \frac{1}{4}\beta b_\gamma + O(\beta^3). \quad (50)$$

Figure 7 shows the temperature dependence of the spin correlation functions, the decoupling parameter α , and the magnetization m . The temperature dependence of the correlation functions is similar to the case with $m = 0$. However, the angular dependence of the energy and specific heat exhibits notable differences compared to the $m = 0$ case. Figure 8 shows the angular dependence of the correlation functions, magnetization, energy, and specific heat. The energy per site is defined as:

$$E = -\frac{1}{2}J(c_x + c_y + c_z) - m|\mathbf{b}|. \quad (51)$$

The angular dependence of the correlation functions is similar to the $m = 0$ case, where c_γ attains its minimum values at the angles where $\tilde{b}_\gamma = 0$. The angular dependence of the magnetization, m , simply reflects the direction of the magnetic field. Despite the similarity in the angular dependence of the correlation functions between the $m = 0$ and finite magnetization cases, the angular dependence of the energy and specific heat shows significant differences. Specifically, the periodicity changes from 60° to 180° . A 180° periodicity is observed for different magnetic fields, as shown in Fig. 9. This result suggests that to observe the 60° periodicity in the specific heat, the effect of the magnetization must be suppressed.

V. SUMMARY

We have investigated the effect of a magnetic field on the Kitaev model using the equation of motion approach for the spin Green's function, considering both cases: $m = 0$ (suppressed magnetization) and $m \neq 0$ (finite magnetization). When magnetization is suppressed, the specific heat exhibits an angular dependence with a 60° periodicity, which is consistent with experimental observations in $\alpha\text{-RuCl}_3$ [25]. This behavior can be interpreted as a signature of Majorana fermion gap formation. However, when magnetization is included, the periodicity shifts from 60° to 180° , suggesting that the Majorana fermion gap behavior is no longer observed. Our analysis therefore indicates that to observe features associated with Majorana fermions, the effect of magnetization must be suppressed. One possible explanation

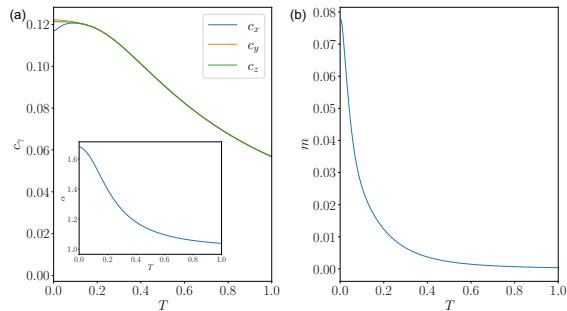


FIG. 7. (a) Temperature dependence of the spin correlation functions c_x , c_y , and c_z . The inset shows the temperature dependence of the decoupling parameter α , introduced in the decoupling approximation. (b) Temperature dependence of the magnetization m . Both (a) and (b) are computed for $b = 0.2$ and $\phi = 40^\circ$.

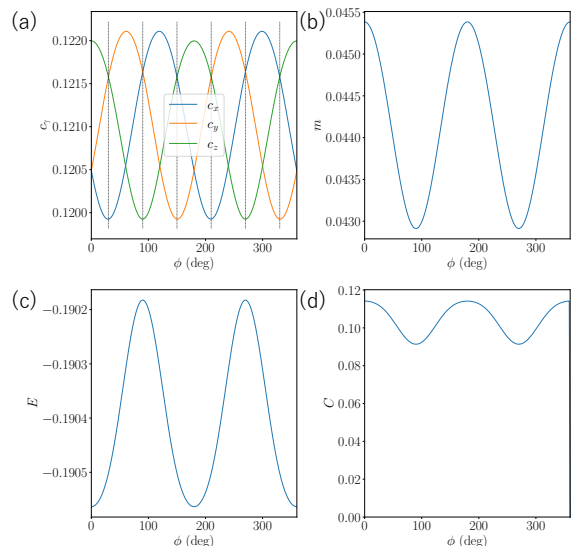


FIG. 8. (a) Spin correlation functions c_x , c_y , and c_z , (b) magnetization m , (c) energy, and (d) specific heat as functions of angle ϕ . The vertical lines indicate specific angles as described earlier. The magnetic field is $b = 0.2$ and the temperature is $T = 0.05$.

is that non-Kitaev interactions[18, 42–44], such as the antiferromagnetic Heisenberg interaction, could suppress the magnetization effect, leading to a regime where Majorana fermion physics becomes relevant. Investigating this scenario would require extending our analysis to incorporate these additional interactions. Another possible scenario is the antiferromagnetic Kitaev interaction, where the effect of magnetization is naturally suppressed due to antiferromagnetic correlations between nearest-neighbor spins. In fact, previous studies [30, 32, 35] have suggested that the spin liquid phase extends further in the antiferromagnetic Kitaev case compared to the ferromagnetic case. Extending our analysis to include non-Kitaev

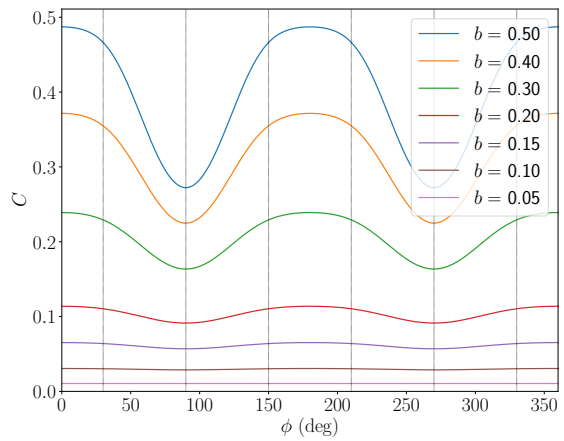


FIG. 9. Angular dependence of the specific heat at $T = 0.05$ for various magnetic field strengths. The vertical lines mark the specific angles as described earlier.

interactions and exploring the case of the antiferromagnetic Kitaev interaction remain important directions for future research.

Appendix A: Algorithm for Solving the Green's Function Equation

In this appendix, we describe how to solve the equations for the Green's functions in the form of Eq. (24). In general, we need to solve the following equation for $\mathbf{G}(i\omega_n)$:

$$i\omega_n \mathbf{G}(i\omega_n) = M \mathbf{G}(i\omega_n) + \mathbf{c}, \quad (\text{A1})$$

where M is an $m \times m$ matrix, \mathbf{c} is an m -dimensional vector, and $\mathbf{G}(i\omega_n)$ has the following form:

$$\mathbf{G}(i\omega_n) = \begin{pmatrix} G_1(i\omega_n) \\ G_2(i\omega_n) \\ \vdots \\ G_m(i\omega_n) \end{pmatrix}. \quad (\text{A2})$$

Let λ_ℓ and \mathbf{v}_ℓ ($\ell = 1, 2, \dots, m$) be the eigenvalues and eigenvectors of the matrix M , respectively, satisfying:

$$M \mathbf{v}_\ell = \lambda_\ell \mathbf{v}_\ell. \quad (\text{A3})$$

If the eigenvectors \mathbf{v}_ℓ are linearly independent, then $\mathbf{G}(i\omega_n)$ can be expanded as:

$$\mathbf{G}(i\omega_n) = \sum_{\ell=1}^m C_\ell(i\omega_n) \mathbf{v}_\ell. \quad (\text{A4})$$

The coefficient $C_\ell(i\omega_n)$ is determined by substituting this equation into Eq. (A1). This yields:

$$C_\ell(i\omega_n) = \sum_{\ell'=1}^m \frac{(V^{-1})_{\ell\ell'} (\mathbf{v}_{\ell'}^* \cdot \mathbf{c})}{i\omega_n - \lambda_\ell}. \quad (\text{A5})$$

Here, the components of the matrix V are defined as: $V_{\ell\ell'} = \mathbf{v}_\ell^* \cdot \mathbf{v}_{\ell'}$. Thus, from Eq. (A4), we obtain:

$$\mathbf{G}(i\omega_n) = \sum_{\ell=1}^m \frac{\mathbf{v}_\ell (V^{-1})_{\ell\ell'} (\mathbf{v}_{\ell'}^* \cdot \mathbf{c})}{i\omega_n - \lambda_\ell}. \quad (\text{A6})$$

-
- [1] A. Kitaev, Anyons in an exactly solved model and beyond, *Ann. Phys.* **321**, 2 (2006).
- [2] A. Kitaev, Fault-tolerant quantum computation by anyons, *Ann. Phys.* **303**, 2 (2003).
- [3] C. Nayak, S. H. Simon, A. Stern, M. Freedman, and S. Das Sarma, Non-Abelian anyons and topological quantum computation, *Rev. Mod. Phys.* **80**, 1083 (2008).
- [4] J. Alicea, New directions in the pursuit of Majorana fermions in solid state systems, *Rep. Prog. Phys.* **75**, 076501 (2012).
- [5] X.-Y. Feng, G.-M. Zhang, and T. Xiang, Topological Characterization of Quantum Phase Transitions in a Spin-1/2 Model, *Phys. Rev. Lett.* **98**, 087204 (2007).
- [6] H.-D. Chen and J. Hu, Exact mapping between classical and topological orders in two-dimensional spin systems, *Phys. Rev. B* **76**, 193101 (2007).
- [7] H.-D. Chen and Z. Nussinov, Exact results of the Kitaev model on a hexagonal lattice: spin states, string and brane correlators, and anyonic excitations, *J. Phys. A: Math. Theor.* **41**, 075001 (2008).
- [8] S. M. Winter, A. A. Tsirlin, M. Daghofer, J. van den Brink, Y. Singh, P. Gegenwart, and R. Valentí, Models and materials for generalized Kitaev magnetism, *J. Phys.: Condens. Matter* **29**, 493002 (2017).
- [9] H. Takagi, T. Takayama, G. Jackeli, G. Khaliullin, and S. E. Nagler, Concept and realization of Kitaev quantum spin liquids, *Nat. Rev. Phys.* **1**, 264 (2019).
- [10] S. Trebst and C. Hickey, Kitaev materials, *Phys. Rep.* **950**, 1 (2022).
- [11] S. Kim, B. Yuan, and Y.-J. Kim, α -RuCl₃ and other Kitaev materials, *APL Mater.* **10**, 080903 (2022).
- [12] G. Jackeli and G. Khaliullin, Mott Insulators in the Strong Spin-Orbit Coupling Limit: From Heisenberg to a Quantum Compass and Kitaev Models, *Phys. Rev. Lett.* **102**, 017205 (2009).
- [13] P. A. Maksimov and A. L. Chernyshev, Rethinking α -RuCl₃, *Phys. Rev. Research* **2**, 033011 (2020).
- [14] R. D. Johnson, S. C. Williams, A. A. Haghighirad, J. Singleton, V. Zapf, P. Manuel, I. I. Mazin, Y. Li, H. O. Jeschke, R. Valentí, and R. Coldea, Monoclinic crystal structure of α -RuCl₃ and the zigzag antiferromagnetic ground state, *Phys. Rev. B* **92**, 235119 (2015).
- [15] J. A. Sears, M. Songvilay, K. W. Plumb, J. P. Clancy, Y. Qiu, Y. Zhao, D. Parshall, and Y.-J. Kim, Magnetic order in α -RuCl₃: A honeycomb-lattice quantum magnet with strong spin-orbit coupling, *Phys. Rev. B* **91**, 144420 (2015).
- [16] S. M. Winter, Y. Li, H. O. Jeschke, and R. Valentí, Challenges in design of Kitaev materials: Magnetic interactions from competing energy scales, *Phys. Rev. B* **93**, 214431 (2016).
- [17] S.-H. Do, S.-Y. Park, J. Yoshitake, J. Nasu, Y. Motome, Y. Kwon, D. T. Adroja, D. J. Voneshen, K. Kim, T.-H. Jang, J.-H. Park, K.-Y. Choi, and S. Ji, Majorana fermions in the Kitaev quantum spin system α -RuCl₃, *Nat. Phys.* **13**, 1079 (2017).
- [18] J. G. Rau, E. K.-H. Lee, and H.-Y. Kee, Generic Spin Model for the Honeycomb Iridates beyond the Kitaev Limit, *Phys. Rev. Lett.* **112**, 077204 (2014).
- [19] R. Yadav, N. A. Bogdanov, V. M. Katukuri, S. Nishimoto, J. van den Brink, and L. Hozoi, Kitaev exchange and field-induced quantum spin-liquid states in honeycomb α -RuCl₃, *Sci. Rep.* **6**, 37925 (2016).
- [20] A. Banerjee, P. Lampen-Kelley, J. Knolle, C. Balz, A. A. Aczel, B. Winn, Y. Liu, D. Pajerowski, J. Yan, C. A. Bridges, A. T. Savici, B. C. Chakoumakos, M. D. Lumsden, D. A. Tennant, R. Moessner, D. G. Mandrus, and S. E. Nagler, Excitations in the field-induced quantum spin liquid state of α -RuCl₃, *npj Quantum Materials* **3**, 8 (2018).
- [21] Y. Kasahara, T. Ohnishi, Y. Mizukami, O. Tanaka, S. Ma, K. Sugii, N. Kurita, H. Tanaka, J. Nasu, Y. Motome, T. Shibauchi, and Y. Matsuda, Majorana quantization and half-integer thermal quantum Hall effect in a Kitaev spin liquid, *Nature* **559**, 227 (2018).
- [22] T. Yokoi, S. Ma, Y. Kasahara, S. Kasahara, T. Shibauchi, N. Kurita, H. Tanaka, J. Nasu, Y. Motome, C. Hickey, S. Trebst, and Y. Matsuda, Half-integer quantized anomalous thermal Hall effect in the Kitaev material candidate α -RuCl₃, *Science* **373**, 568 (2021).
- [23] M. Yamashita, J. Gouchi, Y. Uwatoko, N. Kurita, and H. Tanaka, Sample dependence of half-integer quantized thermal Hall effect in the Kitaev spin-liquid candidate α -RuCl₃, *Phys. Rev. B* **102**, 220404 (2020).
- [24] J. A. N. Bruin, R. R. Claus, Y. Matsumoto, N. Kurita, H. Tanaka, and H. Takagi, Robustness of the thermal Hall effect close to half-quantization in α -RuCl₃, *Nat. Phys.* **18**, 401 (2022).
- [25] O. Tanaka, Y. Mizukami, R. Harasawa, K. Hashimoto, K. Hwang, N. Kurita, H. Tanaka, S. Fujimoto, Y. Matsuda, E.-G. Moon, and T. Shibauchi, Thermodynamic evidence for a field-angle-dependent Majorana gap in a Kitaev spin liquid, *Nat. Phys.* **18**, 429 (2022).
- [26] P. Czajka, T. Gao, M. Hirschberger, P. Lampen-Kelley, A. Banerjee, J. Yan, D. G. Mandrus, S. E. Nagler, and N. P. Ong, Oscillations of the thermal conductivity in the spin-liquid state of α -RuCl₃, *Nat. Phys.* **17**, 915 (2021).
- [27] P. Czajka, T. Gao, M. Hirschberger, P. Lampen-Kelley, A. Banerjee, N. Quirk, D. G. Mandrus, S. E. Nagler, and N. P. Ong, Planar thermal Hall effect of topological bosons in the Kitaev magnet α -RuCl₃, *Nat. Mater.* **22**, 36 (2022).
- [28] L. Janssen and M. Vojta, Heisenberg–Kitaev physics in magnetic fields, *J. Phys.: Condens. Matter* **31**, 423002 (2019).

- [29] J. Das, S. Kundu, A. Kumar, and V. Tripathi, Field tuning Kitaev systems for spin fractionalization and topological order, *J. Phys.: Condens. Matter* **36**, 443001 (2024).
- [30] C. Hickey and S. Trebst, Emergence of a field-driven U(1) spin liquid in the Kitaev honeycomb model, *Nat. Commun.* **10**, 530 (2019).
- [31] D. A. S. Kaib, S. M. Winter, and R. Valentí, Kitaev honeycomb models in magnetic fields: Dynamical response and dual models, *Phys. Rev. B* **100**, 144445 (2019).
- [32] Z. Zhu, I. Kimchi, D. N. Sheng, and L. Fu, Robust non-Abelian spin liquid and a possible intermediate phase in the antiferromagnetic Kitaev model with magnetic field, *Phys. Rev. B* **97**, 241110 (2018).
- [33] Y.-F. Jiang, T. P. Devereaux, and H.-C. Jiang, Field-induced quantum spin liquid in the Kitaev-Heisenberg model and its relation to α -RuCl₃, *Phys. Rev. B* **100**, 165123 (2019).
- [34] N. D. Patel and N. Trivedi, Magnetic field-induced intermediate quantum spin liquid with a spinon fermi surface, *Proc. Natl. Acad. Sci.* **116**, 12199 (2019).
- [35] M. Gohlke, R. Moessner, and F. Pollmann, Dynamical and topological properties of the Kitaev model in a [111] magnetic field, *Phys. Rev. B* **98**, 014418 (2018).
- [36] H.-Y. Lee, R. Kaneko, L. E. Chern, T. Okubo, Y. Yamaji, N. Kawashima, and Y. B. Kim, Magnetic field induced quantum phases in a tensor network study of Kitaev magnets, *Nat. Commun.* **11**, 1639 (2020).
- [37] H. Takegami and T. Morinari, Spin-Spin Correlations in the Kitaev Model at Finite Temperatures: Approximate and Exact Results via Green's Function Equation of Motion, *J. Phys. Soc. Jpn.* **93**, 083703 (2024).
- [38] H. Takegami and T. Morinari, Static and dynamical spin correlations in the Kitaev model at finite temperatures via Green's function equation of motion, *Phys. Rev. B* **111**, 054413 (2025).
- [39] Y. Motome and J. Nasu, Hunting Majorana Fermions in Kitaev Magnets, *J. Phys. Soc. Jpn.* **89**, 012002 (2020).
- [40] S. Tyablikov and V. Bonch-Bruевич, Perturbation theory for double-time temperature-dependent Green functions, *Adv. Phys.* **11**, 317 (1962).
- [41] J. Kondo and K. Yamaji, Green's-Function Formalism of the One-Dimensional Heisenberg Spin System, *Progr. Theoret. Phys.* **47**, 807 (1972).
- [42] J. Chaloupka, G. Jackeli, and G. Khaliullin, Kitaev-Heisenberg Model on a Honeycomb Lattice: Possible Exotic Phases in Iridium Oxides A₂IrO₃, *Phys. Rev. Lett.* **105**, 027204 (2010).
- [43] Y. Singh, S. Manni, J. Reuther, T. Berlijn, R. Thomale, W. Ku, S. Trebst, and P. Gegenwart, Relevance of the Heisenberg-Kitaev Model for the Honeycomb Lattice Iridates A₂IrO₃, *Phys. Rev. Lett.* **108**, 127203 (2012).
- [44] H.-S. Kim and H.-Y. Kee, Crystal structure and magnetism in α -RuCl₃: An ab initio study, *Phys. Rev. B* **93**, 155143 (2016).